
Article:
Mandle, Richard orcid.org/0000-0001-9816-9661, Stock, Nina, Cowling, Stephen James orcid.org/0000-0002-4771-9886 et al. (4 more authors) (2019) Condensation of free volume in structures of nematic and hexatic liquid crystals. LIQUID CRYSTALS. pp. 114-123. ISSN 1366-5855

https://doi.org/10.1080/02678292.2018.1475686

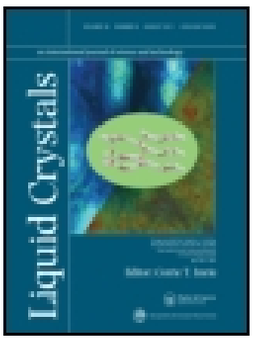

Liquid Crystals

ISSN: 0267-8292 (Print) 1366-5855 (Online) Journal homepage: http://www.tandfonline.com/loi/tlct20

Condensation of free volume in structures of nematic and hexatic liquid crystals

Richard J Mandle, Nina Stock, Stephen J Cowling, Rachel R Parker, Sam Hart, Adrian C Whitwood & John W Goodby

To cite this article: Richard J Mandle, Nina Stock, Stephen J Cowling, Rachel R Parker, Sam Hart, Adrian C Whitwood & John W Goodby (2018): Condensation of free volume in structures of nematic and hexatic liquid crystals, Liquid Crystals, DOI: 10.1080/02678292.2018.1475686

To link to this article: https://doi.org/10.1080/02678292.2018.1475686

Published online: 23 May 2018.

LIQUID CRYSTALS
https://doi.org/10.1080/02678292.2018.1475686

Taylor & Francis
Taylor & Francis Group

Condensation of free volume in structures of nematic and hexatic liquid crystals

Richard J Mandle, Nina Stock, Stephen J Cowling, Rachel R Parker, Sam Hart, Adrian C Whitwood and John W Goodby

Department of Chemistry, The University of York, York, UK

ABSTRACT

Eight novel liquid crystalline materials were prepared containing highly branched terminal chains, either 2,4,4-trimethylpentyl or 3,5,5-trimethylhexyl. All materials exhibit nematic mesophases, with additional smectic (Sm) C, hexatic B and SmI phases for certain homologues. Analysis by small- and wide-angle X-ray scattering reveals continual build-up of the correlation length within the nematic phases, where we also observe splitting of the small angle peak into four lobes, indicating pretransitional Sm fluctuations. Connoscopy confirms the nematic phase to be uniaxial and optically positive. We observe that in the solid state, the molecules exist as staggered antiparallel pairs as a consequence of the sterically demanding bulky terminal group, and this would also appear to manifest in the hexatic B phase, where the layer spacing was found to be greater than the molecular length. If true, this is an example of pair formation driven by sterics rather than dipole–dipole interactions and suggests that reentrant systems driven purely by steric frustration may be found.

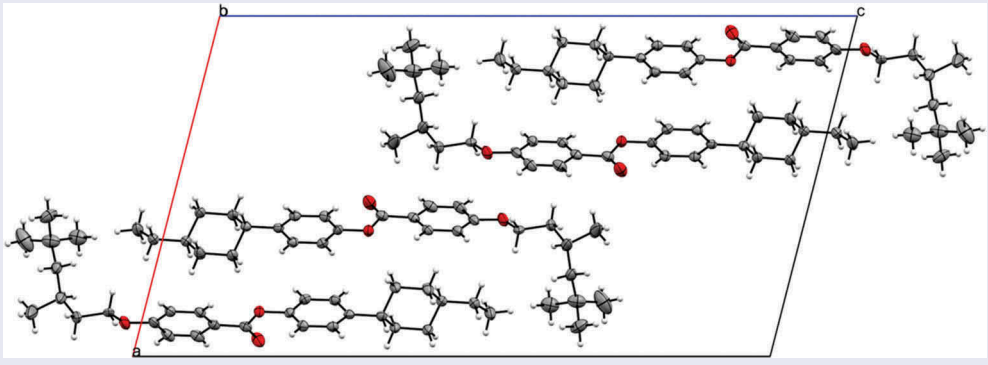

ARTICLE HISTORY
Received 22 March 2018
Accepted 9 May 2018

KEYWORDS
Liquid crystals; SAXS; hexatic phases; smectic phases

Introduction

Ferroelectric liquid crystals have the potential to out-perform nematic liquid crystals in electrooptic devices [1]. They exhibit faster response times, excellent viewing angles and bistable operation [2], Due to a lack of materials with desirable properties (e.g. birefringence [3], alignment, tilt angles and resistivities), this technology is as yet unrealised on mass scale [4–14]. Optimisation of one parameter can be to the detriment of others, for example, birefringence can be lowered by incorporating cyclohexyl rings *in lieu* of phenyl at the cost of reduced phase stability and tilt angle. Previous studies demonstrated that by incorporating bulky groups into the peripheral aliphatic chains of materials that exhibited smectic (Sm) C/C* phases, it is possible to enhance mesophase temperature ranges and suppress melting points [9–14]. Additionally, halogen terminal groups have been reported to stabilise lamellar phases in some systems [15], but not in others [16]. These studies favour the Wulf steric model [17] of the SmC phase as opposed to the McMillan polar theory [18,19]. Thus, in this work, materials with combinations of cyclohexyl units and branched peripheral chains were targeted for the synthesis of ferroelectric hosts combining low birefringence high Sm-phase stability and low melting points.

The compound hexyl 4-pentyloxybiphenyl-4′-carboxylate (65OBC) [20] was shown to be a member of a family of esters that exhibited a SmB phase which did not possess long-range periodic ordering of its constituent molecules. This material was shown by small- and wide-angle X-ray scattering (SWAXS) to exhibit a stacked hexatic B phase [21,22], which was the first

CONTACT Richard J Mandle richard.mandle@york.ac.uk
Supplementary data can be accessed here.

example of a liquid crystal phase to be associated with two-dimensional melting behaviour as predicted by Halperin and Nelson [23] and the preceding work of Kosterlitz and Thouless [24,25]. Hexatic phases were thus predicted to possess long-range two-dimensional (2D) orientational order coupled with short-range positional ordering. As these systems existed in three-dimensional (3D)-condensed phases, they were termed 3D-stacked hexatic phases [26,27] and were classified as Sms B, F and I. In this study, we examine the effects of the inclusion of terminal branching units in the aliphatic chains on the interlayer interactions and the resulting structures of the condensed phases that are formed.

Experimental

The eight compounds uitilised in this work were prepared as depicted in Scheme 1. The one-pot Mitsunobu reaction between methyl 4-hydroxybenzoate (**1**) and either 2,4,4-trimethylpentanol (TMP, **2**) or 3,5,5-trimethylhexanol (**3**) followed by basic hydrolysis afforded the benzoic acids **4** and **5** in high yield over two steps. The subsequent Steglich esterification of **4** and **5** with the *trans* 4-alkylcyclohexylphenols **6–9** furnished compounds **10–17** in high yield and chemical purity as evidenced by reverse-phase high performance liquid chromatography (RP-HPLC) assay.

Quantum chemical calculations were performed using the Gaussian 09 revision e.01 suite of programmes [28]. The small-angle X-ray scattering set-up used is described elsewhere [26]. Single-crystal diffraction data were collected at 110 K on an Oxford Diffraction SuperNova diffractometer with Cu-K_α radiation (λ = 1.54184 Å′ using an EOS CCD camera, see Supplementary data for full details. The atomistic and configurational structures of representative materials from both series were confirmed via X-ray diffraction on single crystals of compounds **10** and **14** grown in a thermal gradient in neat ethanol, see Figure 5 and Figure SI-2. Both materials are all *trans* with a single *gauche* dihedral in the chain connecting the bulky group to the mesogenic core.

Results

We first examined the thermal behaviour of the TMP (compounds **10–13**)-terminated materials; transition temperatures and enthalpies of transition are presented in Table 1. Phase identification was made by polarised

Table 1. Transition temperatures (T, °C) and associated enthalpies (ΔH) for compounds **10–13** as determined by DSC at a heat/cool rate of 10°C min^{-1}.

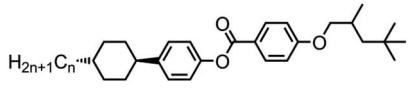

No.	m		MP	SmB-N	N-Iso
10	2	T	76.2	–	83.0
		ΔH	17.2	–	0.1
11	3	T	80.5	–	109.3
		ΔH	43.9	–	0.8
12	4	T	61.4	51.5	99.3
		ΔH	33.3	3.0	0.3
13	5	T	78.9	57.6	106.5
		ΔH	23.9	2.8	0.6

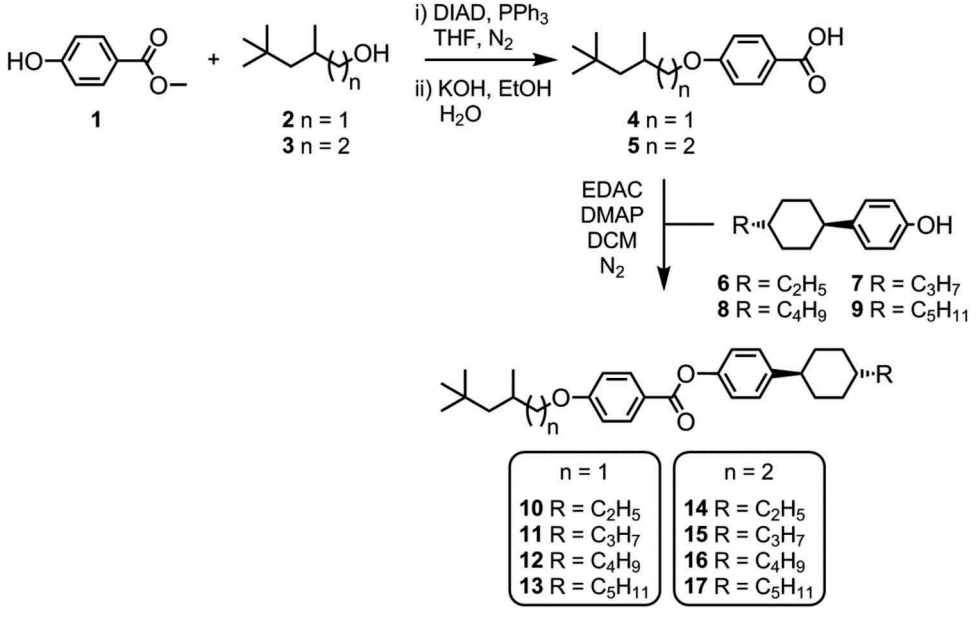

Scheme 1.

Table 2. Transition temperatures (T, °C) and associated enthalpies (ΔH) for compounds **14–17** as determined by DSC at a heat/cool rate of 10°C min^{-1}.

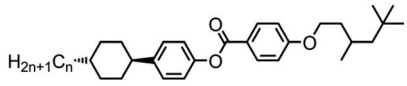

No.	m		MP	SmI-SmC	SmC-N	N-Iso
14	2	T	68.3	–	–	92.1
		ΔH	35.6	–	–	0.3
15	3	T	86.8	–	–	120.7
		ΔH	26.1	–	–	0.3
16	4	T	80.8	–	42.8	112.9
		ΔH	24.6	–	0.8	0.4
17	5	T	76.9	37.0	50.5	119.2
		ΔH	19.0	0.4	1.1	0.4

optical microscopy and assisted with SWAXS. Transition temperatures and associated enthalpies of transition were determined by differential scanning calorimetry (DSC) at a heat/cool rate of 10°C min^{-1} and are the average of two runs.

Compounds **10–13**l exhibit enantiotropic nematic phases, with **12** and **13** exhibiting a monotropic SmB phase on cooling. However, the optical textures of the SmB phase (Figure 1(b)) were not of the typical mosaic kind usually observed for the crystal B variant. Instead, the lancets were curved, suggesting the phase-lacked extensive long-range ordering that would be present in a crystal B phase and suggesting that it is a hexatic B phase. It should be noted that the natural texture of the hexatic B phase has hitherto not been seen, as the defect textures observed have been derived paramorphotically from the SmA phase. Photomicrographs of the nematic and Sm phases of compounds **13** are given in Figure 1.

We studied compounds **12** and **13** by X-ray scattering; representative two-dimensional SWAXS patterns are given in Figure 1(c,d). The small-angle scattering in the nematic phase is split into four lobes of equal intensity; azimuthal averaging of each frame in the range $2\theta = 0.6–2$ gave scattering intensity versus χ, allowing us to determine the angle between the connected lobes to be a constant 70° (see Supplemental data, Figure **SI-2**). This four-lobe pattern arises from cybotactic domains within the nematic phase whose constituent molecules are tilted away from the layer normal analogous to the SmC phase [29]. The SmB phases of both **12** and **13** were unaglined by the magnetic field, even when slowly cooled (1°C min^{-1}) from the nematic phase. Due to the short range of supercooling, it was not possible to obtain scattering patterns more than 2°C below the N-SmB phase transition for **12**, whereas **13** typically crystallised unless the sample was rapidly cooled into the SmB phase. The SmB layer spacing of **12** was determined to be 30.0 Å, giving a d/l ratio of 1.12 when using the molecular length obtained from the B3LYP/6-31G(d) minimised geometry of **12**

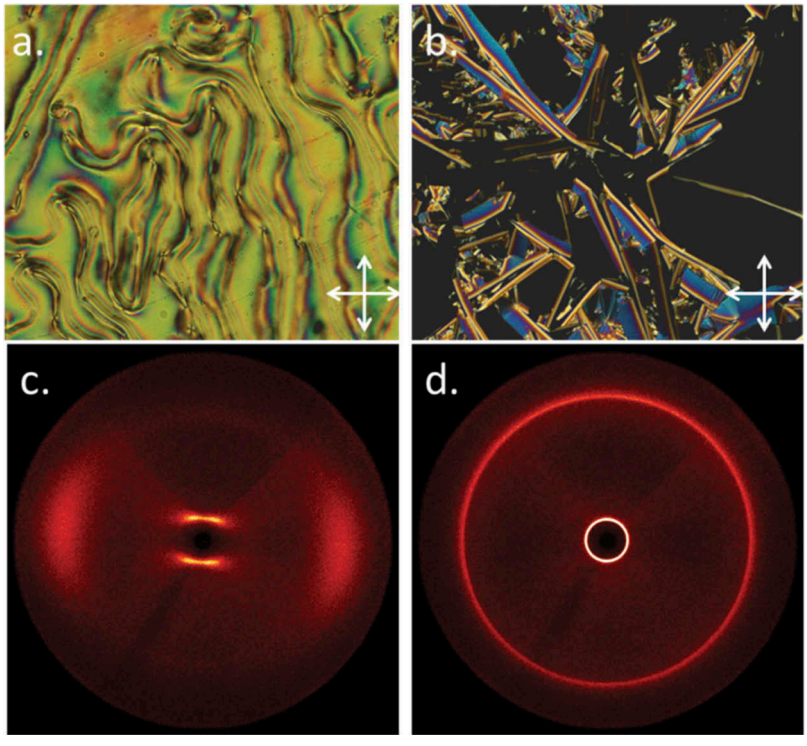

Figure 1. (Colour online) Photomicrographs (100×) of the *schlieren* texture of the nematic phase of compound **13** (a, 104°C), the curved lancet texture of the SmB phase of compound **13** along with homeotropic regions (b). 2D SWAXS patterns of (c) the magnetically aligned nematic phase of **13** at 76°C, (d) an unaligned sample of the SmB phase of **13** at 50°C.

(26.8 Å). Similarly, the SmB layer spacing of **13** was determined to be 31 Å, affording a d/l ratio of 1.12 when using the minimised geometry of **13** (27.6 Å). The fact that both compounds have layer spacings that are slightly greater than the molecular length necessitates an interdigitated structure, a point we will return to shortly. As shown in Figure 3(b), the B phase exhibits optically extinct regions due to homeotropic alignment; if the molecules were tilted within the layers, a *schlieren* texture would be observed, as seen for compound **17** in the SmC/SmI phases (Figure 3(c,d)).

Compounds **14**–**17** (Table 2) were all found to exhibit enantiotropic nematic phases. Whereas the longer homologues of the 2,4,4-trimethylpentlyloxy series exhibit a SmB phase, we find compounds **16** and **17** to exhibit tilted Sm phases. Tentative assignment as SmC and SmI was made based on the presence of four brush singularities in their *schlieren* textures (Figure 2(a,b)) These observations exclude the possibility of the presence of anticlinic phases, which exhibit additional two-brush defects. Therefore, the two phases are drawn from the SmC or hexatic I and F groups. POM indicated that the phases were SmC and SmI and this was confirmed by construction of a phase diagram between **17** and terepthalylidene-bis-p-n-decylaniline (TBDA) – the SmF phase was suppressed whereas the SmC and SmI phases were miscible at all concentrations (Supplemental data, Figure SI-3).

The structures of tilted Sm phases of **16** and **17** formed sequentially on cooling from the nematic phase were investigated by variable temperature small- and wide-angle X-ray scattering (VT-SWAXS) in applied magnetic fields. The two-dimensional X-ray scattering patterns for the aligned compound **17** are exemplified in Figure 2 for the SmC phase and the SmI phase. The SmC phase exhibited only a first-order reflection, whereas the SmI phase showed an additional second-order reflection, indicating the presence of long-range order perpendicular to the layer planes for the I phase in comparison to that of the SmC phase. Additionally, the scattering at wide angles was found to increase in both intensity and definiton upon entering

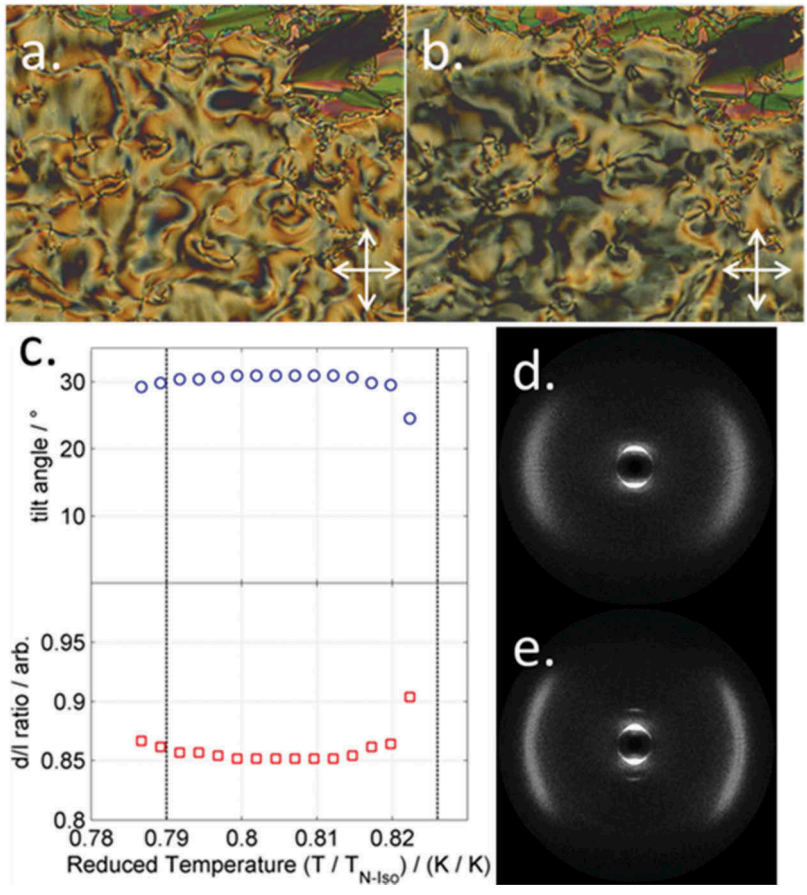

Figure 2. (Colour online) Photomicrographs (100×) of the *schlieren* and fan textures of the SmC phase of **17** (a, 49.7°C), and *schlieren* and fan textures of the SmI phase of **17** (b, 34.6°C). Plot of tilt angle (c, top) and layer spacing as a d/l ratio (c, bottom) for compound **17**, the dashed lines corresponding to the N–SmC and SmC–SmI transitions, respectively. Two-dimensional SWAXS frames for a magnetically aligned sample of **17** in the SmC (d, 49°C) and SmI phases (e, 35°C) .

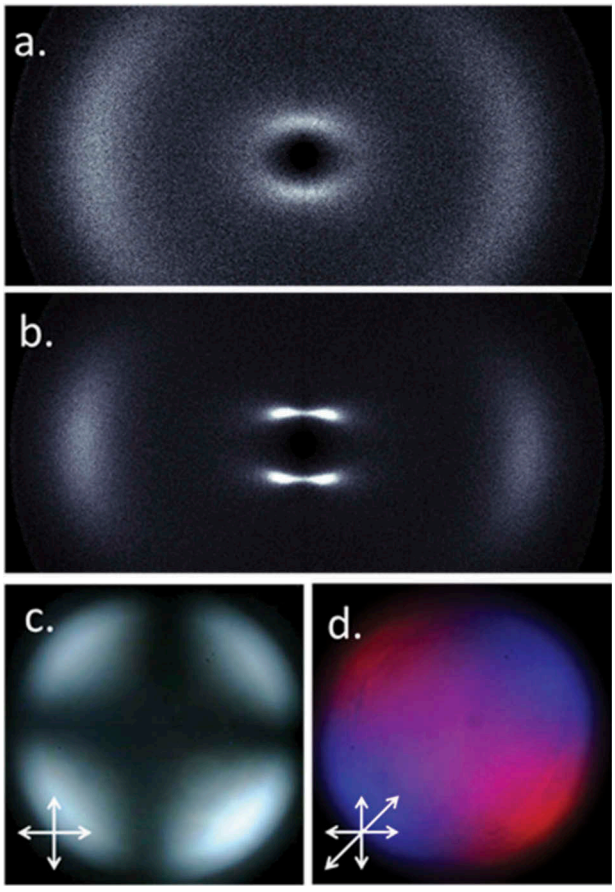

Figure 3. (Colour online) (a) 2D SWAXS pattern of the nematic phase of **17** at 115°C; (b) 2D SWAXS pattern of the nematic phase of **17** at 63°C; (c) conoscopic figure obtained for the nematic phase of compound **17** sandwiched between glass treated with trichlorooctadecylsilane to give homeotropic alignment; (d) insertion of a ¼ waveplate allows determination of the optic sign as positive.

the SmI phase, indicating an increase in organisation within the plane of the layers.

The alignment of the SmC and I phases of compound **17** in the applied magnetic field allowed the tilt angle to be determined assuming that the terminal bulky units were not interferring in packing at the layer interfaces. In the SmC phase, the layer spacing was observed to plateau at 25.4 Å, thereby giving a d/l ratio of 0.86 when using the molecular length obtained for the B3LYP/6-31G(d) minimised geometry of **17** (29.7 Å). The layer spacing was found to increase in the SmI phase to give a maximum value of 27.0 Å prior to crystallisation, i.e. a d/l ratio of 0.91. Thus, the tilt angle in the SmC phase reached saturation at 30.5° and decreased to 29.0° in the SmI phase, as shown in Figure 2(c). If of course we use estimated molecular lengths obtained by using the comparative layer spacings obtained when the terminal groups are excluded, as in the B phase, the tilt angles will be slightly larger.

When studied by VT-SWAXS, the nematic phases of compounds **12, 13** and **17** were found to exhibit unremarkable scattering patterns close to the clearing point (Figure 3(a)). Upon futher cooling, the diffuse small-angle scattering peak splits into four lobes of aproximately equal intensity (Figure 3(b)). The angle of offset within the lobes is temperature independent and takes a value of 70°. The splitting of the small angle scattering peak into four lobes is a consequence of pretransitional Sm fluctuations [30,31]. As shown in Figure 3(c,d), conoscopy demonstrates the nematic phase of **17** to be uniaxial and optically positive. We note that the conoscopic figure does not change across the entire nematic phase range.

The two principal methods for determination of the tilt angle of fluid spectic phases are X-ray scattering and optical measurements. However, these two methods give significantly different results as the results from X-ray diffraction are due to the tilt of the entire molecule, whereas optical methods are sensitive to the tilt of the π-aromatic regions in the central molecular core [32]. In the case where a direct N–SmC transition occurs a tilt angle of 45° is usually expected, but in the case of compound **17**, the values obtained by SWAXS are far lower than this value. However, such an outcome is expected for a SmC phase based on the steric Wulf model, wherein the aliphatic chains are aproximately parallel with one another but with the central core being tilted with respect to this axis. If we assume that both alkyl chains are perpendicular to the layer planes, and that only the aromatic core tilts, we can determine an estimated angle between the core and the two aliphatic chains that satisfies the measured d/l ratio. Using molecular lengths obtained at the B3LYP/6-31G(d) level of density functional theory (DFT), it can be calculated that the subdivisions of the molecule (chain-core-chain) have lengths of 8.3 Å, 14.9 Å and 6.1 Å, respectively, as shown in Figure 4; in order to satisfy a layer spacing of 25.4 Å (a d/l ratio of 0.86), such lengths require a chain-core angle of 45°.

The slighly greater layer spacing than the molecular length suggests that the bulky end groups tend to be squeezed into the interfaces between the layers via size exclusion, as similarly reported previously for the SmA phases of substituted cyanobiphenyls [10]. This displacement of sterically demanding end groups into the layer interfaces is similarly manifested in the solid state as shown by the unit cells of **10** and **14** (Figure 5). The formation of antiparallel pairs in strongly polar liquid crystalline materials (e.g. 4-cyanobiphenyls, 4-nitrobiphenyls) [33,34] is a well-known and well-studied phenomenon; however, in the present case, the pairing is driven purely by steric factors. The term 'steric dipole' was introduced by Petrov et al. to

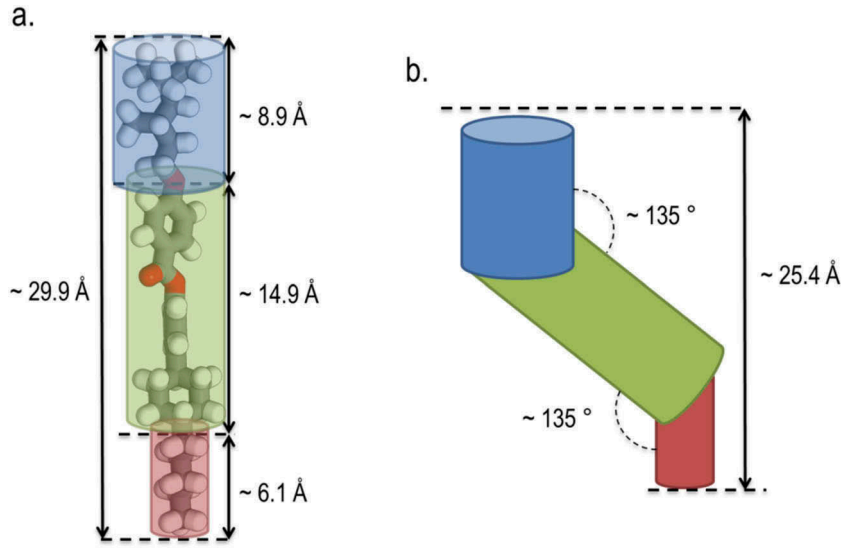

Figure 4. (Colour online) (a) Cartoon depiction of the subdivisions of the molecular structure of compound **17** overlaid atop the B3LYP/6-31G(d) optimised geometry with the molecular length and approximate dimensions of molecular subdivisions indicated and (b) cartoon depiction of the tilt angle between the mesogenic core (green) and the alkyl chains (blue and red), which is required to achieve a layer spacing of 25.4 Å.

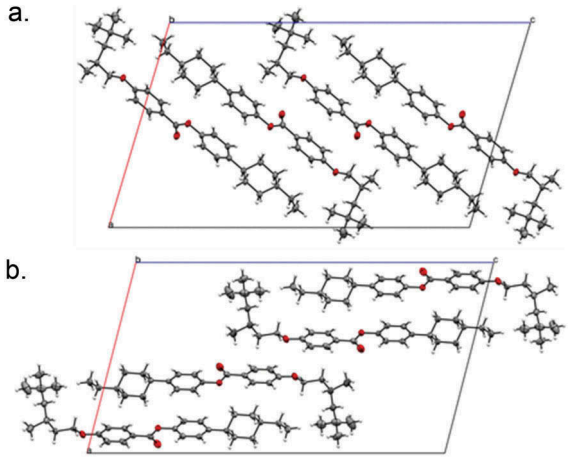

Figure 5. (Colour online) The unit cells of compounds **10** (A, $P2_1/C$ symmetry) and **14** (B, $P2_1/n$ symmetry) displayed with thermal elipsoid model (50% probability level) as obtained by X-ray diffraction on single crystals grown from ethanol with a thermal gradient.

describe the phenomenon of sterically induced pair formation [35], and we reuse this term here. Staggered pair formation through steric factors has been observed in the solid state of polycatenar materials [36], as well as in siloxane terminated compounds via microphase segregation [37–39]. The chemical incompatibility of hydrocarbon and fluorocarbon segments generally leads to bilayer type phases when both are incorporated at opposite ends of a rod-like liquid crystal [40–42], but can also drive pair formation [43,44]. Moreover, the competition between chemical incompatibility between $-CH_2-/-CF_2-$ and steric dipole effects can drive the formation of fluctuated lamellar phases [45] and bicontinuous cubic phases [46]. In the present case, the staggered antiparallel pairing resulting from the incorporation of bulky groups is not accompanied by micro/nanophase segregation due to chemical incompatibility and would therefore appear to be a purely steric phenomenon. It is well known that dipole–dipole antiparallel pairing can lead to re-entrant phase transitions [47], similarly re-entrant behaviour has been observed in polycatenar systems where the pair formation is a consequence of steric factors only [48]. Although we do not observe re-entrant behaviour in the present systems, we expect that such behaviour is possible in rod-like materials whereby the antiparallel pairing is driven by the presence of a single branched alkyl chain, much like the re-entrant behaviour observed in some double-swallow-tailed compounds [49]

We anticipated that if the antiparallel pairing in the solid state (Figure 5) is also found in the liquid crystalline state, there should be some impact on the correlation lengths. For example, in the SmB/I phases, the pairing would probably reduce any possible interdigitation and thus the out-of-plane correlation length might be rather short, whereas the in-plane correlations will take fairly typical values. There is already some evidence for pairing from the SmB layer spacing and the seemingly low SmC tilt angles. We therefore measured the correlation length in-plane and out-of-plane compounds **13** and **17** as follows. A Voigt fit to the raw scattering data was used

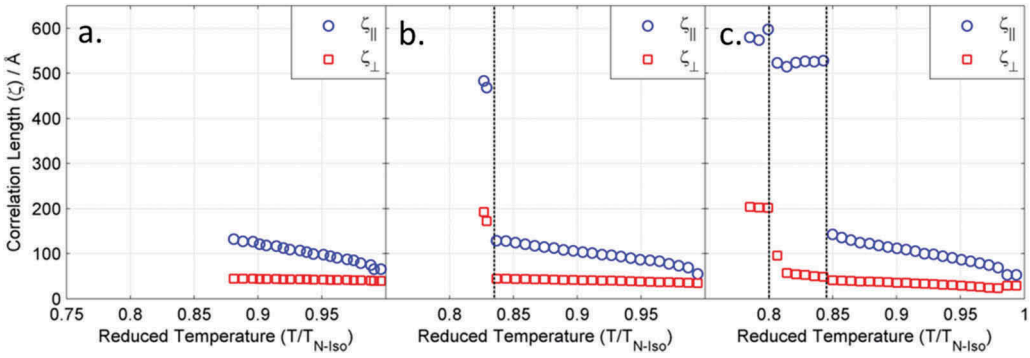

Figure 6. (Colour online) Correlation lengths parallel ($\zeta_{||}$, Å) and perpendicular ($\zeta_{\perp}$, Å) to the director for compounds **12** (a),**13** (b) and **17** (c) determined by SWAXS as described in the text. Dashed lines correspond to phase transitions.

to determine the full width at half maximum (FWHM) for both the wide- and small-angle scattering peaks, this was corrected for instrumental broadening against a sample of silver behenate, purchased from TCI chemicals [50]. From the FWHM, we obtain the correlation length, which is plotted as a function of reduced temperature ($T/T_{N\text{-}Iso}$, K/K) in Figure **6**. For each material, there is a continuous increase in correlation length parallel to the director across the entire nematic phase ring, while the value perpendicular to the director remains constant. For **13**, both correlation lengths increase sharply at the N–SmB phase transition to ~500 Å and ~200 Å, respectively, consistent with those reported for the hexatic phase of hexyl pentyloxybiphenyl-4-carboxylate 65OCB [21,22]. Crystallisation of the sample prevented obtaining values in the SmB phase of **12**; however, the increase in both in-plane and out-of-plane correlation lengths across the nematic phase range is comparable to that of **13**. Whereas the hexatic B phase, the phase under examination has only short to quasi-long range in-plane positional order, the crystal B phase has long-range positional ordering both parallel and perpendicular to the director. Thus, measurement of correlation length supports the assignment as a hexatic B phase (i.e. SmB_{hex}) rather than a crystal B phase, this is supported by the relatively small enthalpy value of the N–SmB transition (3.0 kJ mol^{-1}).

For **17**, the correlation length perpendicular to the director increases to ~500 Å at the N–SmC transition whereas perpendicular to the director there is a more modest increase, supporting the assignment as a fluid Sm phase. At the SmC–SmI transition, there is a small increase in the out-of-plane correlation length to ~600 Å, while the in-plane correlation jumps to ~200 Å. Such values are consistent with the absence of hexatic packing in the SmC phase and the onset of hexatic packing in the SmI phase.

These results indicate that the nematic phases exhibit increasing fluctuations of the lower temperature phases as the first-order phase transitions to SmB or SmC phases approach upon cooling, and that the fluctuations can be observed in temperature ranges well beyond these phase transitions. In the SmB and SmI phases, the in-plane correlation lengths are quasi-long range, as expected for hexatic phases, whereas for the SmC phase of **17**, they are only marginally larger than those of the nematic phase. After the transition into a Sm phase, the out-of-plane correlation length increases sharply, thus out-of-the-plane organisation can be considered a quasi-one-dimensional crystal, based upon the repeats of the layers. However, due to the screening between the layers due to the bulky end groups, translation of the local packing arrangements between layers is unlikely. Thus, the bond orientational ordering in the B and I phases is probably contained within the layers and is not translated between layers and therefore the B and I phases are probably 2D, rather than stacked 3D hexatic phases as described in the studies on the first hexatic liquid crystal 65OBC.

Discussion

We have presented eight novel liquid crystalline materials composed of a 4-(4-alkylcyclohexyl)phenyl benzoate mesogenic unit and featuring one of two highly branched terminal chains (2,4,4-trimethylpentyloxy or 3,5,5-trimethylhexyloxy). All eight materials exhibit enantiotropic nematic phase, with longer homologues exhibiting either SmB (**12** and **13**) or SmC (**16**) or SmC and SmI (**17**) phases. When studied by small-angle X-ray scattering, we find that the layer spacings of the SmB phases are larger (i.e. not commensurate) with the molecular lengths (obtained at the B3LYP/6-31G(d) level of DFT), one explanation for this is that there is a degree of staggered antiparallel correlation of adjacent molecules (i.e. pair formation through steric effects). Compounds **10** and **14** were studied by X-ray

diffraction on single crystals, and we observe staggered antiparallel packing in the solid state of both materials. We predict that this phenomenon could be exploited to lead to further examples of re-entrant phase transition driven entirely by shape segregation of molecules, and we note that some potential examples of this type of behaviour have been reported in calamitics [51–54] along with experimentally confirmed examples in polycatenar materials [48]. For the SmC and SmI phases of **17**, the layer spacing is somewhat less than the molecualr length, as expected for a tilted Sm phase.

Melting in 2D was described in the work of Berezinski, Kosterliz and Thouless (BKT), where BKT transitions can be found in 2D systems that are approximated by an XY model, including Josephson junction arrays, thin disordered superconducting granular films and 2D superconductor-insulator transitions [55]. In the 2D XY model for disordered phases with differing correlations, a second-order phase transition is not predicted. However, a low-temperature quasi-ordered phase with a correlation function that decays orderly with distance and temperature is predicted [56]. The transition from the high-temperature disordered phase with the exponential correlation (such as a nematic-like phase) to a low-temperature quasi-ordered phase (such as a SmB) is a transition of infinite order. Halperin and Nelson developed this theory to include 2D melting in liquid crystal films [23], and the first 3D analogue was found in 65OBC where the local hexagonal packing array of the molecules was not extended over long distances, but decayed geometrically [22]. However, the orientation of the local hexagonal array extended over long distances in 3D and was termed 'bond-orientational order'. The screening out of the interlayer interactions in the B and I phases of the materials described indicates that they may be examples of 2D hexatics. As with the twist grain boundary phases, the 2D hexatics share some of the same fundamental properties and structures with those of superconductors.

Acknowledgments

We would like to thank the Engineering and Physical Sciences Research Council (EPSRC) for support of this work via grant codes EP/K039660/1 and EP/M020584/1, and Dr. E. J. Davis for useful discussions. Crystal structures of **10** and **14** have been deposited with the CCDC. Raw data are available upon request from the University of York data catalogue. The authors thank the referee for constructive advice and comments during the peer review process.

Disclosure statement

No potential conflict of interest was reported by the authors.

Funding

This work was supported by the Engineering and Physical Sciences Research Council [grant codes EP/K039660/1 and EP/M020584/1].

ORCID

Richard J Mandle http://orcid.org/0000-0001-9816-9661
Stephen J Cowling http://orcid.org/0000-0002-4771-9886
Rachel R Parker http://orcid.org/0000-0002-3767-3888
Adrian C Whitwood http://orcid.org/0000-0002-5132-5468

References

[1] Goodby JW. The nanoscale engineering of nematic liquid crystals for displays. Liq Cryst. 2011;38(11–12):1363–1387. PubMed PMID: WOS:000297464800004.
[2] Clark NA, Lagerwall ST. Submicrosecond bistable electro-optic switching in liquid-crystals. Appl Phys Lett. 1980;36(11):899–901. PubMed PMID: WOS:A1980JV22600009.
[3] Dong CC, Styring P, Goodby JW, et al. The synthesis and electro-optic properties of liquid crystalline 2-(2,3-difluorobiphenyl-4 '-yl)-1,3-dioxanes. J Mater Chem. 1999;9(8):1669–1677. PubMed PMID: WOS:000081920600005.
[4] Hird M, Goodby JW, Hindmarsh P, et al. The design, synthesis and structure-property relationships of ferroelectric and antiferroelectric liquid crystal materials. Ferroelectrics. 2002;276:219–237. PubMed PMID: WOS:000178789500020.
[5] Kusumoto T, Hiyama T, Takehara S. Design and synthesis of chiral dopants having a chiral ring structure for ferroelectric liquid-crystals. Nippon Kagaku Kaishi. 1992;(12):1401–1411. PubMed PMID: WOS:A1992KD11300001.
[6] Walba DM, Sierra T, Rego JA, et al. Controlling the structure of ferroelectric liquid-crystal thin-films by design - the molecules to materials connection. Abstr Pap Am Chem S. 1991;202:202–Biot. PubMed PMID: WOS:A1991HG08000709.
[7] Goodby JW, Leslie TM. Ferroelectric liquid-crystals - structure and design. Mol Cryst Liq Cryst. 1984;110(1–4):175–203. PubMed PMID: WOS:A1984TQ29400014.
[8] Hird M. Ferroelectricity in liquid crystals-materials, properties and applications. Liq Cryst. 2011;38(11–12):1467–1493. PubMed PMID: WOS:000297464800010.
[9] Mandle RJ, Davis EJ, Sarju JP, et al. Control of free volume through size exclusion in the formation of smectic C phases for display applications. J Mater Chem C. 2015;3(17):4333–4344. PubMed PMID: WOS:000353769300017.
[10] Mandle RJ, Davis EJ, Voll CCA, et al. Self-organisation through size-exclusion in soft materials. J Mater Chem C. 2015;3(10):2380–2388. PubMed PMID: WOS:000350693200027.
[11] Mulligan KM, Bogner A, Song QX, et al. Design of liquid crystals with 'de Vries-like' properties: the effect of carbosilane nanosegregation in 5-phenyl-1,3,4-thiadiazole mesogens. J Mater Chem C. 2014;2(39):8270–8276. PubMed PMID: WOS:000342881600009.

[12] Schubert CPJ, Bogner A, Porada JH, et al. Design of liquid crystals with 'de Vries-like' properties: carbosilane-terminated 5-phenylpyrimidine mesogens suitable for chevron-free FLC formulations. J Mater Chem C. 2014;2(23):4581–4589. PubMed PMID: WOS:000336834400009.

[13] Roberts JC, Kapernaum N, Giesselmann F, et al. Design of liquid crystals with "de Vries-like" properties: organosiloxane mesogen with a 5-phenylpyrimidine core. J Am Chem Soc. 2008;130(42):13842–13843. PubMed PMID: WOS:000260047700016.

[14] Thompson M, Carkner C, Bailey A, et al. Tuning the mesogenic properties of 5-alkoxy-2-(4-alkoxyphenyl) pyrimidine liquid crystals: the effect of a phenoxy end-group in two sterically equivalent series. Liq Cryst. 2014;41(9):1246–1260. PubMed PMID: WOS:000338705100004.

[15] Rupar I, Mulligan KM, Roberts JC, et al. Elucidating the smectic A-promoting effect of halogen end-groups in calamitic liquid crystals. J Mater Chem C. 2013;1(23):3729–3735. PubMed PMID: WOS:000319360700015.

[16] Davis EJ, Mandle RJ, Russell BK, et al. Liquid-crystalline structure-property relationships in halogen-terminated derivatives of cyanobiphenyl. Liq Cryst. 2014;41(11):1635–1646. PubMed PMID: WOS:000344456600017.

[17] Wulf A. Steric model for the smectic-C phase. Phys Rev A. 1975;11(1):365–375.

[18] McMillan WL. Simple molecular theory of the smectic C phase. Phys Rev A. 1973;8(4):1921–1929.

[19] Madhusudana NV. Dipolar origin of tilting of rod-like molecules in the smectic C phase. Liq Cryst. 2015;42(5–6):840–863. PubMed PMID: WOS:000358163400022.

[20] Goodby JW, Pindak R. Characterization of the hexatic-B and crystal B-phases by optical microscopy. Mol Cryst Liq Cryst. 1981;75(1–4):233–247. PubMed PMID: WOS:A1981MP91000020.

[21] Pindak R, Moncton DE, Davey SC, et al. X-ray-observation of a stacked hexatic liquid-crystal B-phase. Phys Rev Lett. 1981;46(17):1135–1138. PubMed PMID: WOS:A1981LL72100007.

[22] Moncton DE, Pindak R, Davey SC, et al. X-ray observations of a stacked hexatic liquid-crystal B-phase. B Am Phys Soc. 1981;26(3):274–275. PubMed PMID: WOS:A1981LE30500485.

[23] Nelson DR, Halperin BI. Dislocation-mediated melting in two dimensions. Phys Rev B. 1979;19(5):2457–2484.

[24] Kosterlitz JM. Commentary on 'Ordering, metastability and phase transitions in two-dimensional systems' J M Kosterlitz and D J Thouless (1973 J-Phys. C: solid State Phys. 6 1181-203)-the early basis of the successful Kosterlitz-Thouless theory. J Phys-Condens Mat. 2016;28(48). PubMed PMID: WOS:000385448700001. DOI:10.1088/0953-8984/28/48/481001

[25] Kosterlitz JM, Thouless DJ. Ordering, metastability and phase transitions in two-dimensional systems. J Phys C: Solid State Phys. 1973;6(7):1181.

[26] Huang CC, Viner JM, Pindak R, et al. Heat-capacity study of the transition from a stacked-hexatic-B phase to a smectic-a phase. Phys Rev Lett. 1981;46(19):1289–1292. PubMed PMID: WOS:A1981LN61200011.

[27] Noh DY, Brock JD, Litster JD, et al. Fluid, hexatic, and crystal phases in terephthal-bis-(4\textit{n})-alkylanilines. Phys Rev B. 1989;40(7):4920–4927.

[28] Frisch MJ, Trucks GW, Schlegel HB, et al. Gaussian 09, Revision A.02, 2009. Wallingford(CT), Gaussian, Inc.,

[29] Vaupotic N, Szydlowska J, Salamonczyk M, et al. Structure studies of the nematic phase formed by bent-core molecules. Phys Rev E. 2009;80(3). Pub Med PMID: WOS:000270383400010. DOI:10.1103/PhysRevE.80.030701

[30] Vries AD. X-ray photographic studies of liquid-crystals .4. isotropic, nematic, and smectic a phases of some 4-alkoxybenzal-4′-ethylanilines. Mol Cryst Liq Cryst. 1973;20(2):119–131. PubMed PMID: WOS:A1973P271900003.

[31] Azaroff LV. X-ray-scattering by cybotactic nematic mesophases. Proc Natl Acad Sci United States America-Physical Sci. 1980;77(3):1252–1254. PubMed PMID: WOS:A1980JL81000007.

[32] Cowling SJ, Hall AW, Goodby JW, et al. Examination of the interlayer strength of smectic liquid crystals through the study of partially fluorinated and branched fluorinated end-groups. J Mater Chem. 2006;16(22):2181–2191. PubMed PMID: WOS:000237951700009.

[33] Mandle RJ, Cowling SJ, Sage I, et al. Relationship between molecular association and re-entrant phenomena in polar calamitic liquid crystals. J Phys Chem B. 2015;119(7):3273–3280. PubMed PMID: WOS:000349942300049.

[34] Mandle RJ, Cowling SJ, Goodby JW. Evaluation of 4-alkoxy-4 '-nitrobiphenyl liquid crystals for use in next generation scattering LCDs. Rsc Adv. 2017;7(64):40480–40485. PubMed PMID: WOS:000408043100051.

[35] Petrov AG, Derzhanski A. Generalized asymmetry of thermotropic and lyotropic mesogens. Mol Cryst Liq Cryst. 1987;151:303–333. PubMed PMID: WOS:A1987L824000025.

[36] Cardinaels T, Ramaekers J, Nockemann P, et al. Rigid tetracatenar liquid crystals derived from 1,10-phenanthroline. Soft Matter. 2008;4(11):2172–2185. PubMed PMID: WOS:000261733100009.

[37] Ibnelhaj M, Skoulios A, Guillon D, et al. Structural characterization of linear dimeric and cyclic tetrameric liquid-crystalline siloxane derivatives. Liq Cryst. 1995;19(3):373–378. PubMed PMID: WOS:A1995RV31100013.

[38] Corsellis E, Guillon D, Kloess P, et al. Structural characterization of mono- and di-mesogenic organosiloxanes: the impact of siloxane content on biphenyl benzoate systems. Liq Cryst. 1997;23(2):235–239. PubMed PMID: WOS:A1997XN08800009.

[39] Tschierske C. Non-conventional liquid crystals - the importance of micro-segregation for self-organisation. J Mater Chem. 1998;8(7):1485–1508. PubMed PMID: WOS:000074812100001.

[40] Hopken J, Moller M. On the morphology of (perfluoroalkyl)alkanes. Macromolecules. 1992;25(9):2482–2489. PubMed PMID: WOS:A1992HR58600029.

[41] Viney C, Russell TP, Depero LE, et al. Transitions to liquid-crystalline phases in a semifluorinated alkane. Mol Cryst Liq Cryst. 1989;168:63–82. PubMed PMID: WOS:A1989U118300006.

[42] Nguyen HT, Sigaud G, Achard MF, et al. Rod-like mesogens with antipathetic fluorocarbon and hydrocarbon tails. Liq Cryst. 1991;10(3):389–396. PubMed PMID: WOS:A1991GB00800009.

[43] Bilgin-Eran B, Yorur C, Tschierske C, et al. Liquid crystals based on semiperfluorinated imines and salicylaldimato metal complexes. A comparative study of alkyl, alkoxy and polyether substituents. J Mater Chem. 2007;17(22):2319–2328. PubMed PMID: WOS:000247349400017.

[44] Gainar A, Tzeng MC, Heinrich B, et al. Incompatibility-driven self-organization in polycatenar liquid crystals bearing both hydrocarbon and fluorocarbon chains. J Phys Chem B. 2017;121(37):8817–8828. PubMed PMID: WOS:000411772100020.

[45] Imai M, Kawaguchi A, Saeki A, et al. Fluctuations of lamellar structure prior to a lamellar -> gyroid transition in a non-ionic surfactant system. Phys Rev E. 2000;62(5):6865–6874. PubMed PMID: WOS:000165341900023.

[46] Yamaguchi A, Uehara N, Yamamoto J, et al. Lamellar to lamellar phase transition driven by conformation change of an amphiphilic liquid crystal oligomer. Chem Mater. 2007;19(26):6445–6450. PubMed PMID: WOS:000251733600016.

[47] Cladis PE, Guillon D, Bouchet FR, et al. Reentrant nematic transitions in cyano-octyloxybiphenyl (8OCB). Phys Rev A. 1981;23(5):2594–2601.

[48] Pietrasik U, Szydlowska J, Krowczynski A, et al. Re-entrant isotropic phase between lamellar and columnar mesophases. J Am Chem Soc. 2002;124(30):8884–8890. PubMed PMID: WOS:000177074400037.

[49] Weissflog W, Letko I, Pelzl G, et al. Re-entrant isotropic behaviour of a pure double-swallow-tailed compound. Liq Cryst. 1995;18(6):867–870.

[50] Huang TC, Toraya H, Blanton TN, et al. X-ray-powder diffraction analysis of silver behenate, a possible low-angle diffraction standard. J Appl Crystallogr. 1993;26:180–184. PubMed PMID: WOS:A1993KY85100005.

[51] Mandle RJ, Cowling SJ, Goodby JW. Rational design of rod-like liquid crystals exhibiting two nematic phases. Chem-Eur J. 2017;23(58):14554–14562. PubMed PMID: WOS:000413167100023.

[52] Mandle RJ, Cowling SJ, Goodby JW. A nematic to nematic transformation exhibited by a rod-like liquid crystal. Phys Chem Chem Phys. 2017;19(18):11429–11435. PubMed PMID: WOS:000401022300045.

[53] Sasaki T, Takanishi Y, Yamamotob J, et al. A frustrated phase driven by competition among layer structures. Soft Matter. 2017;13(30):5194–5203. PubMed PMID: WOS:000407069700011.

[54] Kishikawa K, Yamamoto Y, Watanabe G, et al. Shape-assisted self-organization in highly disordered liquid crystal phases. Angew Chem Int Edit. 2017;56(16):4598–4602. PubMed PMID: WOS:000398154000036.

[55] Resnick DJ, Garland JC, Boyd JT, et al. Kosterlitz-Thouless transition in proximity-coupled superconducting arrays. Phys Rev Lett. 1981;47(21):1542–1545. PubMed PMID: WOS:A1981MQ50100015.

[56] McBryan OA, Spencer T. On the decay of correlations inSO(n)-symmetric ferromagnets. Commun Math Phys. 1977;53(3):299–302.